The Journal of NUCLEAR MEDICINE

Reversible Extraskeletal Uptake of Bone Scanning in Primary Hyperparathyroidism

Geum Ju Hwang, Jong Doo Lee, Chang Yun Park and Sung Kil Lim

J Nucl Med. 1996;37:469-471.

The Journal of Nuclear Medicine is published monthly.
SNMMI | Society of Nuclear Medicine and Molecular Imaging
1850 Samuel Morse Drive, Reston, VA 20190.
(Print ISSN: 0161-5505, Online ISSN: 2159-662X)

SNMMI SOCIETY OF NUCLEAR MEDICINE AND MOLECULAR IMAGING

neurotoxicity typically occurs within the first month of therapy, but it has been identified several months into the course of treatment. Cyclosporine-induced neurotoxicity is not dose-related and has been identified in patients with normal levels (*1,6*).

A constellation of CT and MRI findings has been reported by several authors to be characteristic of cyclosporine-induced neurotoxicity (*5,6*). CT typically demonstrates symmetrical regions of nonenhancing low density within the white matter of the posterior parietal and occipital lobes, with little mass effect. MRI will show symmetrical areas characterized by signal hyperintensity on T2-weighted images, signal hypointensity on T1-weighted images, and by absence of enhancement on postcontrast images. Occasionally, hemorrhage has been reported within such lesions (*5,6*). While involvement of the parieto-occipital lobes is most frequently encountered, reports suggest that white matter in any part of the brain may be affected. These findings may persist for several months despite discontinuation of cyclosporine treatment, and in the face of clinical improvement (*6*).

The presence of the characteristic findings on CT/MR imaging in combination with the most typical clinical manifestations may yield a correct diagnosis; however, the actual incidence of these typical findings remains unknown. Vogt et al. reported that in 40% of patients postliver transplantation, CT was interpreted as normal (*4*). A normal CT or a CT scan which demonstrates a nonspecific white matter abnormality of indeterminate age is not unusual. In such patients, whose neurological presentation may be atypical and whose cyclosporine levels may fall within the normal range, the neurological differential may be problematic.

The demonstration of perfusion abnormalities on SPECT imaging may permit identification of those patients with cyclosporine-induced neurotoxicity and normal CT and MRI studies. The more rapid resolution of the perfusion abnormalities, in comparison with the abnormalities on CT, more accurately paralleled the patient's clinical course. Our patient presented with hypomagnesemia and hypocholesterolemia at the onset of symptoms. Although these abnormalities as well as hypertention and steroid administration have been identified as exacerbating conditions, cause and effect have not been established (*1,3,5,6*), and the etiology of cyclosporine-induced neurotoxicity remains obscure. Demyelination has been suggested as an explanation for the neuroimaging findings, however, scattered pathological reports have failed to support this theory (*6–7*). Truwit et al. have suggested that cyclosporine neurotoxicity may be the consequence of focal vasoconstriction producing usually mild and reversible ischemia. They propose that cyclosporine-induced neurotoxicity is mediated by the release of endothelin, a neuropeptide which is a potent vasoconstrictor (*6*). This claim is supported by the similarity found between the neuroimaging findings in patients with eclampsia and acute hypertensive encephalopathy (conditions in which endothelin is already postulated to have a role) to those neuroimaging findings described in patients with cyclosporine-induced neurotoxicity (*6*). Alternatively, Stein et al. suggest that cyclosporine may produce cerebral vasoconstriction by altering the balance between prostacyclin and thromboxane A_2 substances which have been found to be vasoactive elsewhere in the body (*3*).

CONCLUSION

The demonstration of moderately decreased perfusion on SPECT imaging corresponding to the regions of white matter abnormalities identified on CT and MRI examinations in our patient further supports the hypothesis that these abnormalities reflect an ischemic insult rather than demyelination. Assuming that the SPECT correlates better with the neurological symptoms, it may eliminate prolonged discontinuation of much-needed immunosuppression and the increased risk of organ rejection. Further studies are needed to determine whether SPECT may be used to identify cyclosporine-induced neurotoxicity in patients whose other imaging studies are nondiagnostic.

REFERENCES

1. Bronster DJ, Emre S, Mor E, Sheiner P, Miller CM, Schwartz ME. Neurologic complications of orthotopic liver transplantation. *Mt Sinai J Med* 1994;61:63–69.
2. Rowley HA, Kaku DA, Ascher NL, Roberts JP, Lake JR. Neurologic findings in 100 consecutive liver transplant recipients. *Neurology* 1990;40(suppl):181.
3. Stein DP, Lederman RJ, Vogt DP, Carey WD, Broughan TA. Neurological complications following liver transplantation. *Ann Neurol* 1992;31:644–649.
4. Vogt DP, Lederman RJ, Carey WD, Broughan TA. Neurologic complications of liver transplantation. *Transplantation* 1988;45:1057–1061.
5. De Groen PC, Aksamit AJ, Rakela J, Forbes GS, Krom RAF. Central nervous system toxicity after liver transplantation: the role of cyclosporine and cholesterol. *N Engl J Med* 1987;317:861–866.
6. Truwit CL, Denaro CP, Lake JR, DeMarco T. MRI of reversible cyclosporine A-induced neurotoxicity. *Am J Neuroradiol* 1991;12:651–659.
7. Boon AP, Adams DH, Carey MP, Williams A, McMaster P, Elias E. Cyclosporin-associated cerebral lesions in liver transplantation [Letter]. *Lancet* 1988;1:1457.

Reversible Extraskeletal Uptake of Bone Scanning in Primary Hyperparathyroidism

Geum Ju Hwang, Jong Doo Lee, Chang Yun Park and Sung Kil Lim

Departments of Diagnostic Radiology and Internal Medicine, Yonsei University, Medical College, Seoul, Korea

Metastatic calcification within soft tissue, such as the lung and stomach, is associated with hyperparathyroidism, chronic renal failure, hemodialysis, metastatic neoplasm and hypervitaminosis D. Bone scanning agents variably accumulate within these extraskeletal metastatic calcifications. We report a patient with primary hyperparathyroidism whose bone scan revealed abnormal uptake in the liver, lung, stomach and parathyroid gland followed by complete resolution of extraskeletal uptake less than 1 wk after parathyroidectomy.

Key Words: metastatic calcification; hyperparathyroidism; bone scintigraphy

J Nucl Med 1996; 37:469–471

Received Feb. 14, 1995; revision accepted Jun. 29, 1995.

For correspondence or reprints contact: J.D. Lee, MD, Department of Diagnostic Radiology, Yonsei University, Medical College, 134 Shinchon-dong, Seodaemoon-ku, Seoul, Korea, 120-752.

Since the introduction of the ^{99m}Tc-phosphate compounds, unusual extraosseous accumulations have been reported, in which

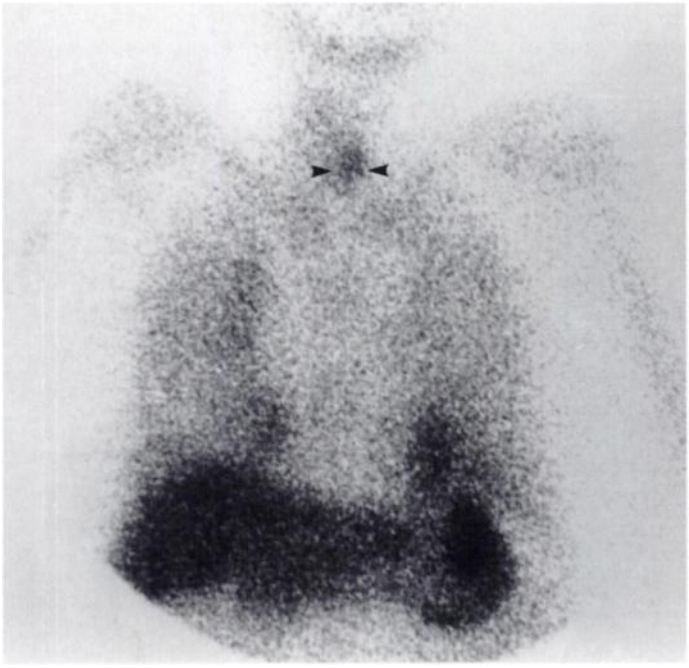

FIGURE 1. Anterior bone scan. Intense accumulation of radioactivity is seen throughout the lung, liver, stomach and left lobe of the thyroid gland.

chemiadsorption into the hydroxyapatite crystals is the proposed mechanism of uptake (*1–4*). The resolution of metastatic calcium deposits of hypercalcemia is somewhat controversial. We recently observed complete reversal of uptake in extraosseous sites (i.e., lung, liver, stomach) in a patient with primary hyperparathyroidism 1 wk after partial parathyroidectomy. Following the resolution of extraskeletal uptake on repeated subsequent postoperative bone scans, an interesting feature occurred: the appearance of intense uptake within the calvarium and mandible which was not demonstrated on the initial bone scan.

CASE REPORT

A 65-yr-old woman was admitted for evaluation of hypercalcemia. Her symptoms consisted of poor oral intake, nausea, fatigue, weight loss (4 kg), indigestion, constipation and polydipsia for 2 wk. On physical examination, a palpable nodule was noted in the neck. The laboratory data at that time showed elevated serum calcium (17.0 mg/dl), serum phosphate (6.6 mg/dl), blood urea nitrogen (59.2 mg/dl), serum creatinine (2.5 mg/dl) and serum alkaline phosphatase (127 mg/dl). Liver function tests were normal. Amino-terminal radioimmunoassay disclosed a serum parathormone concentration of 145.16 pg/ml (normal 10–65 pg/ml). Thyroid test showed a low serum level of the thyroid hormones; T3 32.75 ng/dl (80–220 ng/dl), and FT4 0.76 ng/dl (0.73–1.95 ng/dl). A plain radiograph of the hands showed subperiosteal resorption of the phalanges. A chest radiograph did not reveal any pathologic calcification in bilateral lungs. A CT scan of the neck showed a well-defined 4 × 3 × 2-cm mass on the left lower neck, posterior to the left thyroid gland and medial to the jugular vein. On the basis of the laboratory and CT findings, parathyroid adenoma was diagnosed. A bone scan performed 4 hr after intravenous injection of 20 mCi ^{99m}Tc-MDP revealed increased uptake diffusely throughout the lung, liver, stomach and focally at the left thyroid region (Fig. 1).

Seven days later, a 5 × 2-cm benign adenoma was surgically removed. It was located posterior to the left lobe of the thyroid, originating from the left superior parathyroid and extended to the lower pole of the thyroid. After surgery, serum calcium and phosphorus levels decreased to almost normal ranges (serum calcium, 8.6 mg/dl and phosphate, 3.0 mg/dl). A repeat bone scan 1 wk after the operation exhibited complete disappearance of extraskeletal uptake. Intense uptake at the calvarium, mandible and long bones with faint renal activity was visualized (Fig. 2).

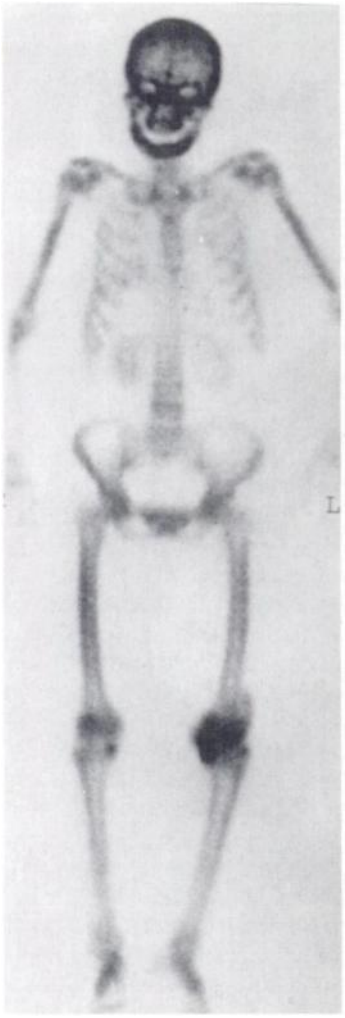

FIGURE 2. Bone scan performed 1 wk after removal of a parathyroid adenoma shows complete resolution of extraskeletal uptake and intense activity in the calvarium, mandible and long bones.

DISCUSSION

Pathologic calcification is classified into two types: dystrophic and metastatic (*5*). Dystrophic calcification occurs after tissue injury in the presence of normal plasma calcium and phosphate concentrations. In contrast, metastatic calcification is calcium deposits within extraskeletal tissues due to abnormal calcium and phosphate metabolism. The etiology of the metastatic calcification includes primary or secondary osteolytic bone tumors, hyperparathyroidism, hypervitaminosis D and chronic renal failure.

In primary hyperparathyroidism, visceral uptake of ^{99m}Tc-labeled phosphate compounds and unusual extraosseous accumulations have been reported. It is generally accepted that the metastatic calcification is predominantly related to an increased Ca × PO_4 product. A rate above 60 seems necessary for the presence of this type of calcification (*6*). In our patient, this product was 112. The affected tissues are either solely those of the lungs (*7,8*) or the lung tissues in association with gastric (*9*), renal (*10*), myocardial (*9,10*) and thyroidal (*9*) uptake. There have been few reports on metastatic calcification to the liver. Our patient showed exceptional metastatic uptake to the liver, in addition to stomach and lung. Moreover, 1 wk after the removal of the tumor resulted in resolution of the extraskeletal uptake and the Ca × PO_4 product was decreased to 25.8. Fundamentally, lower-

ing Ca × PO_4 products by manipulating Ca and PO_4 levels can lead to drastic resolution of these calcifications (*11*). Alfrey et al. (*12*) have already demonstrated radiologically the disappearance of gross tumoral calcifications of chronic uremia after transplantation, either by phosphate supplementation or parathyroidectomy.

We could not correlate the metastatic calcium deposits by bone scan with the anatomic presence of calcification. Radiological diagnosis of diffuse metastatic calcification has proven to be difficult, as the particles are extremely small (microscopic in most cases) (*13*). Lack of MDP uptake by metastatic calcium deposits does not mean the disappearance of the anatomic presence of calcification but represents the metastatic activity of the pathologic calcification.

Among the important bone scintigraphic findings in hyperparathyroidism, uniformly increased bone-to-soft tissue ratios generally associated with faint or absent renal visualization (*14–16*) are a well known classical findings. The mechanism for the super scan is due to low excretion of injected ^{99m}Tc-MDP (10% in 4 hr versus 60% in normal subjects) and a fivefold increase in the total bone-to-soft tissue uptake ratio (*17*). Faint or absent kidney images are due to low soft-tissue activity common to any metabolic bone disease with high bone uptake of ^{99m}Tc-diphosphonate (*11*).

In our patient, the skeletal and renal uptake appeared normal in the first bone scan, whereas the second one, obtained 1 wk after surgery, showed generalized increased activity symmetrically, particularly in the calvarium, the mandible and the diaphysis of long bone (*18*). Relatively higher ^{99m}Tc-MDP uptake in extraskeletal sites may have prevented the appearance of this characteristic feature of hyperparathyroidism in the first bone scan. After surgery, extraskeletal uptake of the radiopharmaceutical decreased, thus allowing the appearance of hyperparathyroidism features on the bone scan.

CONCLUSION

Hepatic, pulmonary and gastric uptake of ^{99m}Tc-MDP could be reversed in primary hyperparathyroidism as the cause of hypercalcemia is resolved. Therefore, the resolution of the extraskeletal metastatic calcification can be correctly assessed with repeat follow-up bone scintigraphy.

REFERENCES

1. Janowitz WR, Serafani AN. Intense myocardial uptake of ^{99m}Tc-diphosphonate in a uremic patient with secondary hyperparathyroidism and pericarditis: case report. *J Nucl Med* 1976;17:896–898.
2. Francis MD. The inhibition of calcium hydroxyapatite crystal growth by polyphosphonates and polyphosphates. *Calcif Tiss Res* 1969;3:151–162.
3. Krane SM, Glindher MJ. Transphosphorylation from nucleoside di- and triphosphates by apatite crystals. *J Biol Chem* 1962;237:2991–2998.
4. Watson NW, Cowan RJ, Maynard D, Richards F. Resolution of metastatic calcification revealed by bone scanning: case report. *J Nucl Med* 1977;18:890–892.
5. Scarpelli DG, Iannaccone PM. Cell injury and errors of metabolism. Kissane JM, ed. In: *Anderson's pathology*. St Louis: Mosby; 1990:1–65.
6. Velentzas C, Meindok H, Oreopoulos DG, et al. Detection and pathogenesis of visceral calcification in dialysis patients and patients with malignant disease. *Can Med Assoc J* 1978;118:45–50.
7. Cohen AM, Maxon HR, Goldsmith RE, et al. Metastatic pulmonary calcification in primary hyperparathyroidism. *Arch Intern Med* 1977;137:520–522.
8. Herry JY, Chevet D, Moison A, et al. Pulmonary uptake of ^{99m}Tc-labeled methylene diphosphonate in a patient with a parathyroid adenoma. *J Nucl Med* 1981;22:888–890.
9. Amico S, Lucas P, Diebold MD, et al. Metastatic calcification in the thyroid gland demonstrated on bone scan in a patient with primary hyperparathyroidism. *J Nucl Med* 1986;27:373–376.
10. Rosenthal DI, Chandler HL, Azizi F, et al. Uptake of bone imaging agents by diffuse pulmonary metastatic calcification. *Am J Roentgenol* 1977;129:871–874.
11. de Jonge FAA, Pauwels EKJ, Hamdy NAT. Scintigraphy in the clinical evaluation of disorders of mineral and skeletal metabolism in renal failure. *Eur J Nucl Med* 1991;18:839–855.
12. Alfrey AC, Jenkins D, Croth CG, et al. Resolution of hyperparathyroidism renal osteodystrophy and metastatic calcification after renal homotransplantation. *N Engl J Med* 1968;279:1349–1356.
13. Mootz JR, Sagel SS, Roberts TH. Roentgenographic manifestations of pulmonary calcifications. A rare cause of respiratory failure in chronic renal disease. *Radiology* 1973;107:55–60.
14. Sy WM, Patel D, Faunce H. Significance of absent or faint kidney sign on bone scan. *J Nucl Med* 1975;16:454–456.
15. Thrupkaew AK, Henkin R, Quinn J. False-negative bone scans in disseminated metastatic disease. *Radiology* 1974;113:383–386.
16. Osmond JD, Pendergrass HP, Potsaxid MS. Accuracy of ^{99m}Tc-diphosphonate bone scans and roentgenograms in the detection of prostate, breast and lung carcinoma metastases. *Am J Roentgenol* 1975;125:972–977.
17. Constable AR, Cranage RW. Recognition of the super scan in prostatic bone scintigraphy. *Br J Radiol* 1981;54:122–125.
18. Sy WM. Bone scan in primary hyperparathyroidism. *J Nucl Med* 1974;15:1089–1091.

Localization of Technetium-99m-Sestamibi in Diffuse Myelodysplastic Processes

Robert E. Reiman and Julie K. Fetters

Departments of Radiology and Medicine, Duke University Medical Center, Durham, North Carolina

We present two patients with skeletal localization of ^{99m}Tc-sestamibi in patients with ringed sideroblastic anemia and polycythemia vera who were undergoing routine myocardial perfusion studies.

Key Words: myelodysplastic disorders; technetium-99m-sestamibi

J Nucl Med 1996; 37:471–473

Technetium-99m-sestamibi (hexakis-2-methoxyisobutylisonitrile ^{99m}Tc(I)) was originally developed as a myocardial perfusion imaging agent and has been widely used in the diagnosis of coronary artery disease since its introduction. It has, however, been shown to preferentially concentrate in a variety of solid tumors. We report the incidental finding of skeletal localization of ^{99m}Tc-sestamibi in two patients with diffuse myelodysplastic processes.

Received Jan. 24, 1995; revision accepted Jun. 17, 1995.

For correspondence or reprints contact: Robert Reiman, MD, Department of Radiology, Box 3808, Duke University Medical Center, Durham, NC 27710.

CASE REPORT

Patient One

A 73-yr-old man was referred for evaluation of a 3-wk history of dyspnea on exertion and palpitations in view of a family history of coronary artery disease. He underwent a myocardial perfusion study utilizing a one-day imaging protocol and received 296 MBq (8.0 mCi) ^{99m}Tc-sestamibi at rest, followed 60 min later by planar imaging in the anterior, 45° LAO and left lateral projections. Imaging was repeated following treadmill exercise using 888 MBq